JOURNAL OF Applied Polymer SCIENCE

Bio-Plastics and Elastomers from Polylactic Acid/Thermoplastic Polyurethane Blends

Vladislav Jašo,[1] Miroslav Cvetinov,[2] Srđan Rakić,[2] Zoran S. Petrović[1]
[1]Kansas Polymer Research Center, Pittsburg State University, Pittsburg, Kansas 66762, USA
[2]Department of Physics, Faculty of Sciences, University of Novi Sad, 21000 Novi Sad, Serbia
Correspondence to: V. Jašo (E-mail: vjaso@pittstate.edu)

ABSTRACT: Blends of two biocompatible polymers: thermoplastic polyester-urethane (TPU) and polylactic acid (PLA) were studied. The effect of the blending ratio on blend morphology and properties was examined by running a series of blends from 10 to 80 wt % of PLA. Increasing TPU concentration in the blends lowered the glass transition and melting point of PLA indicating that the components were compatible and partially miscible. The blends with 10–40 wt % PLA are hard, reinforced elastomers, while those with 60–80 wt % PLA are tough plastics. Cocontinuous morphology was suggested in samples with 40 and 50 wt % PLA. Inversion points between 30 and 40 wt % PLA (from globular phase is dispersed in the matrix to a cocontinuous morphology) and between 50 and 60 wt % PLA (a transition from cocontinuous to TPU dispersed in the PLA matrix) were observed. Elastomers with higher PLA content and intermediate morphology displayed a combination of high tensile strength, hardness, relatively high elongation and modulus. New materials have potential applications in the medical field. © 2014 Wiley Periodicals, Inc. J. Appl. Polym. Sci. **2014**, *131*, 41104.

KEYWORDS: blends; mechanical properties; morphology; polylactic acid; polyurethanes

Received 15 April 2014; accepted 4 June 2014
DOI: 10.1002/app.41104

INTRODUCTION

Polylactic acid (PLA) is one of the commercial bio-based plastic materials offering excellent properties and biodegradability. However, the material is brittle and thus unsuitable for many applications. Increasing toughness of PLA by blending with an elastomer is a useful way to solve the problem. On the other hand, an elastomer can be reinforced by blending with a rigid thermoplastic material.

Both PLA and TPU are biocompatible. They are used in many human clinical applications and are approved by FDA.[1] Some biomedical applications of PLA include surgical sutures, innerfix material of bone fractures, bone screws, bone plates and abdominal mesh.[2] PLA is also used in pharmaceutical applications, especially as matrices for controlled drug delivery.[3–5] TPU is known to be hemocompatible while its flexibility, high strength and toughness, abrasion resistance and biological stability make it an excellent choice for production of medical devices.[1,6–12] It has found applications in blood bags and surgical gloves, as well as in high-risk applications such as catheters, synthetic veins and wound dressings.[13]

Blending PLA with polyethylene[14] and synthetic rubbers[15] proved effective in improving the PLA toughness, but unfortunately, these blends had limited applications because of reduced biodegradability and biocompatibility. To address these issues, toughening of PLA with starch,[16,17] poly (butylene succinate),[18,19] poly (hydroxyalkanoates),[20,21] polymerized soybean oil,[22] and polyamide 11[23] was attempted. These efforts had limited success as most of polymers from renewable resources were less effective than petrochemical-based analogs. TPU is an ideal candidate for toughening PLA, as it has a combination of high strength, elasticity and toughness, as well as biocompatibility and biodegradability. In addition, thermoplastic polyester urethanes should be compatible with PLA, as both have ester bonds in the main chain.[18,19,24] Also, carbamate from hard segments of TPU can form hydrogen bonds with PLA.[6]

Hong et al.[1] have shown that adding TPU elastomer to PLA can gradually transform brittle to ductile fracture. They were able to increase notched impact strength over three times by adding 10 wt % TPU. Bioelastomer (BE) synthesized from biomass diols and diacids significantly increased cold crystallization of PLA.[25] With 11.5 vol % of BE, elongation at break went from 7 to 179% and notched Izod impact strength improved from 2.4 to 10 kJ m^{-2}. Without an obvious drop in the tensile strength, addition of 20 wt % of TPU to PLA raised elongation at break to 350% and notched impact strength to 25 kJ m^{-2}.[26] Elongation was increased even to 602% with 30 wt % TPU while the samples could not be broken in the impact strength test at

room temperature.[6] The tensile strength and modulus of the PLA/TPU blends could be significantly increased by orientation through solid hot drawing. Stress-induced crystallization during drawing was confirmed by increased crystallinity and decreased grain size of PLA.[2] Zhao et al.[2] were able to enhance the blood compatibility of PLA by prolonging kinetic clotting time, and decreasing hemolysis ratio and platelet activation due to the introduction of TPU and orientation of the blend. PLA/TPU (50/50) blends were found to possess unique shape memory properties.[27]

In this study, we explore the effect of composition on morphology and properties of the blends at different PLA/TPU weight ratios. Eight blends with PLA/TPU ratios 80/20, 70/30, 60/40, 50/50, 40/60, 30/70, 20/80, 10/90 were prepared. Mixing two immiscible materials produces a range of morphologies, consisting of two phases varying from the continuous crystalline PLA with dispersed polyurethane globules at low concentration of the elastomer, to co-continuous morphologies at the mid-range of compositions, and continuous elastomeric phase with dispersed rigid rods or globules of PLA at low PLA concentrations. Materials with continuous PLA with dispersed urethanes are expected to have high strength and toughness, whereas those with continuous TPU phase and dispersed PLA would be hard, possibly strong elastomers with good abrasion resistance. Materials with intermediate, co-continuous morphology would be tough plastics of lower modulus and relatively high strength. Polyester soft segments from polyurethane as well as urethane hard segments are expected to be compatible with PLA. The blends should be potentially biodegradable and could find application in the medical field.

Several methods were employed to study these blends and better understand the relationship between their structure and properties. Rheology of blends was studied on a capillary rheometer. Morphology was examined using scanning electron microscopy (SEM) on samples with solvent removed TPU phase and X-ray diffraction (XRD). Thermal properties were characterized using differential scanning calorimetry (DSC) and dynamic mechanical analysis (DMA). Mechanical methods were used to study tensile and elastic properties of blends as well as impact strength.

EXPERIMENTAL

Materials

Elastollan C 60A 10WH (BASF Polyurethanes GmbH, Lemförde, Germany) is a plasticized thermoplastic polyester urethane having nominal Shore A hardness of 64 and density of 1.17 g cm^{-3}.

PLA polymer 6201D (Nature Works, Minnetonka, MN) is a fiber-grade PLA with density 1.24 g cm^{-3} and melt flow index of 15–30 g/10 min (at load 2.16 kg).

Methods

Pellets of the two polymers were weighed and mixed at the appropriate weight ratios and dried for 5 h in a vacuum oven at 80°C. Blending of components was carried out in a Rheomix 600 internal mixer with Rheocord System 40 (HAAKE, Paramus, NJ) at 190°C for 15 min with a rotor speed of 50 RPM. Blends were hot pressed at 190°C into sheets (100 mm × 100 mm × 1 mm) and used for testing.

The viscosity of TPU and PLA at 190°C was determined on Malvern Rosand RH2000 capillary rheometer (Malvern Instruments, Westborough, MA) using the 32-mm long die with 1-mm diameter orifice. Measurements were carried out using twin bore regime, and Bagley correction was applied.

Blend morphology was observed using Phenom scanning electron microscope (Phenom-World BV, Eindhoven, The Netherlands). Samples were cryogenically fractured and surfaces sputter-coated with gold before being studied. Samples were treated with DMF to remove the TPU phase.

X-ray diffraction images were collected on a Gemini S kappa-geometry diffractometer equipped with a Sapphire3 CCD area detector (Agilent Technologies UK, Yarnton, UK) using graphite monochromated Mo Kα ($\lambda = 0.7107$ Å) X-radiation in all measurements. Flat specimens were investigated in transmission geometry, where the sample-to-detector distance was 110 mm.

Measurement of thermal properties was carried out using differential scanning calorimeter (DSC) model Q100 (TA Instruments, New Castle, DE). Measurements were performed in two cycles at a heating/cooling rate of 10°C min^{-1} from −80 to 250°C. Dynamic mechanical analysis (DMA) was carried out on a TA Instruments DMA 2980, at 10 Hz and heating rate of 3°C min^{-1} in a temperature interval from −80 to 120°C.

Mechanical properties (tensile strength, elongation at break) of blends were determined on QTest II tensile tester (MTS Systems, Eden Prairie, MN) at gauge length of 50 mm and extension rate of 50 mm min^{-1}. Shore hardness was determined by Shore A and D durometers (Pacific Transducer, Los Angeles, CA). Izod notched impact properties were determined on Resil Impactor 6957 testing device (Ceast S.p.A., Pianezza, Italy) at ambient temperature. Samples (dimensions 63.5 mm × 12.7 mm × 1 mm) were cut from hot pressed sheets. The specimens were notched up to prescribed depth, using a mechanical notcher. At least five specimens were tested for each sample material to obtain an average value.

RESULTS AND DISCUSSION

Rheology and Morphology of Blends

Viscosity of components affects the morphology and structure of the blends. Viscosity of components was measured at the

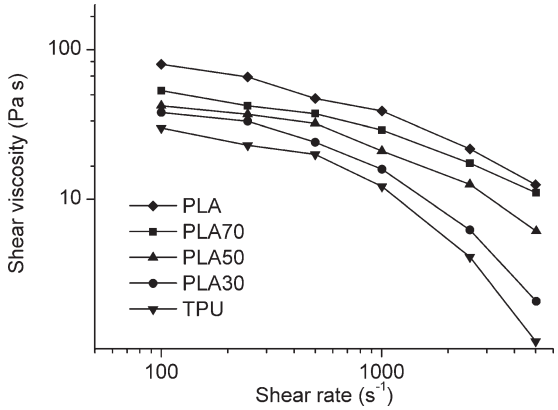

Figure 1. Shear viscosity of pure PLA and TPU and PLA/TPU blends with 70, 50, and 30 wt % of PLA, at 190°C.

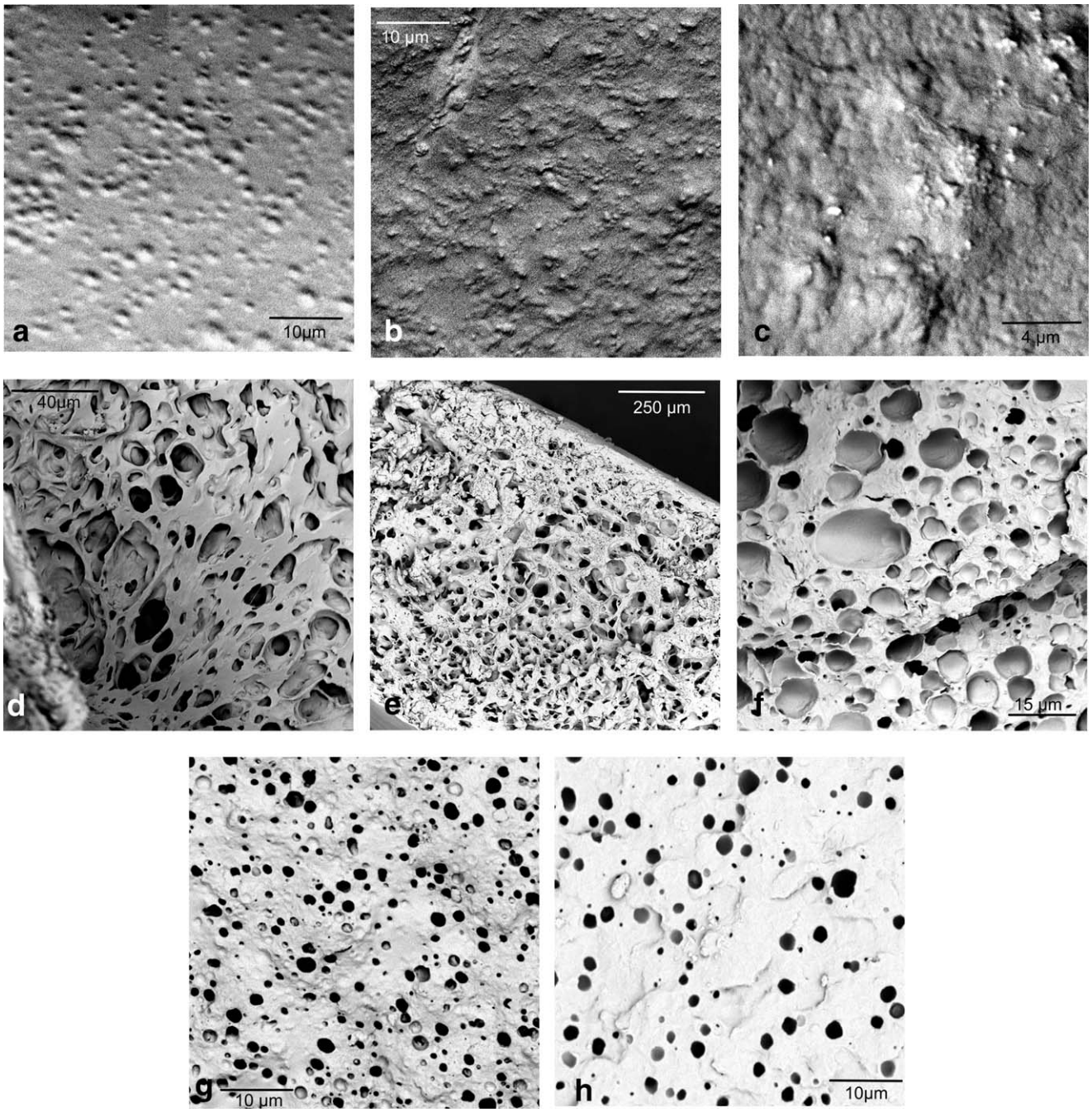

Figure 2. SEM micrographs of the cryogenically fractured surfaces of the PLA/TPU blends treated with DMF to partially remove TPU. 10/90 (a) 20/80 (b), 30/70 (c), 40/60 (d), 50/50 (e), 60/40 (f), 70/30 (g) 80/20 (h).

processing temperature (190°C) as a function of shear rate. PLA had higher viscosity than TPU at this temperature and formed spherical particles in blends with 10–30 wt % PLA. Dependence of shear viscosity versus shear rate is shown in Figure 1. Shear viscosity of blends increases with increasing PLA content. All blends as well as pure components exhibited pseudo-plastic behavior but TPU was the most shear sensitive. The drop of viscosity at higher shear rates was more dramatic in blends with higher wt % of TPU. The dependence of viscosity on blend composition can exhibit linear dependence as well as positive or negative deviation from linearity.[28] We have no data on the miscibility of the components at the processing temperature, but it appears that viscosity of our blends is an additive property.

Morphology was studied on cryogenically fractured samples. Dimethylformamide (DMF) was used to partially dissolve the TPU phase on the surface of cryogenically broken samples in order to better observe the morphology of the blends. Micrographs of surfaces after DMF treatment are shown in Figure 2. In blends with 10, 20, and 30 wt % of PLA, globular structures of a minority PLA phase can be observed [Figure 2(a–c)]. Globules in samples with 10 and 20 wt % of PLA range from 1 to 3

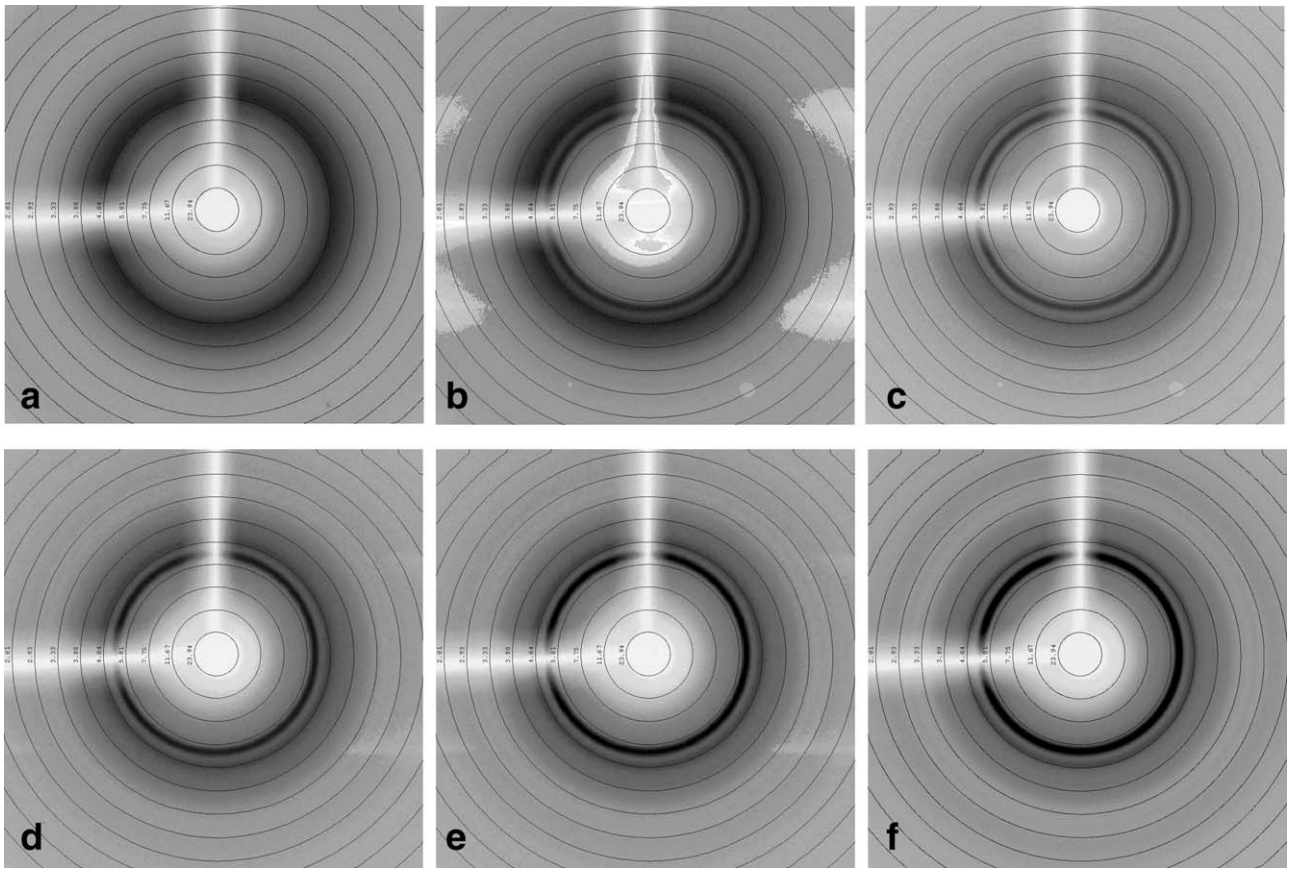

Figure 3. Diffractograms of PLA/TPU blends: 20/80 (a), 30/70 (b), 40/60 (c), 50/50 (d), 60/40 (e), 80/20 (f).

μm. In samples with 30 wt % of PLA, they are in a range from 0.5 to 4 μm. The foamy skeleton of PLA with holes from 2 to 40 μm after TPU removal was observed in Figure 2(d). This suggests a cocontinuous morphology in sample with 40 wt % of PLA. The blend with 50 wt % of PLA had a spongy PLA structure after the removal of TPU [Figure 2(e)] suggesting a co-continuous morphology as well. Globular morphology with dispersed TPU particles in PLA matrix was again observed in samples with 60, 70, and 80 wt % PLA. The removal of the TPU phase in the sample with 60 wt % of PLA [Figure 2(f)] reveals holes with sizes ranging from 2 to 20 μm. Samples with 70 and 80 wt % PLA [Figure 2(g,h)] also exhibited regularly distributed holes with sizes from 1 to 3 μm that remained after the extraction of TPU phase.

X-ray Diffraction

Possible orientation of PLA phase was examined by X-ray diffraction. All diffractograms (Figure 3) exhibit one clear ring and one more diffuse ring. Rings do not form arches which indicate that there is no orientation in any sample, irrespective of

Table I. Transition Temperatures, Heats of Crystallization and Melting, Crystallinity of Pure Polymers and their Blends (First Heating Cycle)

PLA/TPU	T_g (°C); TPU	T_g (°C); PLA	T_c (°C) PLA	T_m (°C); PLA	ΔH_c (J g^{-1}); PLA	ΔH_m (J g^{-1}); PLA	Crystallinity (%)
0/100 TPU	−45.6	-	-	-	-	-	-
10/90	−46.4	-	68.9	155.4	1.09	4.19	33.3
20/80	−45.9	27.4	72.0	157.7	3.50	9.45	31.9
30/70	−46.3	28.0	78.5	159.9	1.15	12.07	39.1
40/60	−44.4	34.0	78.9	160.5	5.45	16.42	29.4
50/50	−44.1	37.3	78.3	161.9	5.77	21.79	34.4
60/40	−43.0	45.4	84.9	165.3	12.21	26.81	26.2
70/30	-	47.2	86.7	166.4	17.05	31.05	21.5
80/20	-	52.7	90.9	166.9	23.18	38.55	20.7
100/0 PLA	-	63.1	111.2	172.7	17.84	32.42	15.7

Table II. Transition Temperatures, Heats of Crystallization and Melting, Crystallinity of Pure Polymers and their Blends (Second Heating Cycle)

PLA/TPU	T_g (°C); TPU	T_g (°C); PLA	T_c (°C); PLA	T_m (°C); PLA	ΔH_c (J g^{-1}); PLA	ΔH_m (J g^{-1}); PLA
0/100 TPU	−45.6	-	-	-	-	-
10/90	−45.7	23.9	75.9	153.8	0.53	1.32
20/80	−44.4	27.6	84.4	156.4	3.05	4.93
30/70	−42.3	30.4	82.5	157.5	8.57	11.95
40/60	−40.6	32.0	77.3	158.4	9.85	15.53
50/50	−40.5	34.0	87.5	161.6	14.70	20.15
60/40	−40.2	41.9	89.9	163.2	17.32	24.51
70/30	-	45.6	91.3	164.1	21.22	28.46
80/20	-	49.2	94.9	165.1	27.73	35.61
100/0 PLA	-	60.8	135.5	167.1	11.72	16.58

morphology. The clearer ring becomes more visible as concentration of PLA in the blend increases reflecting the semicrystalline structure of the PLA phase.

Thermal Properties

Thermal properties measured by DSC offer insight into the interaction between components in the blends. DSC curves of the blends show a glass transition of TPU at −45°C, the second glass transition at around 50°C (PLA), followed by crystallization peaks of PLA at 70–90°C and PLA melting peaks around 160°C. Results of the thermal analysis in DSC are summarized in Tables I and II. Pure TPU had glass transition at around −45°C and PLA at around 67°C. Pure PLA melts at 176°C. The glass transition of PLA is considerably affected by the addition of TPU, while the glass transition of TPU phase changes very little with the addition of PLA. The TPU used for this study is a segmented polymer consisting of hard urethane segments and soft polyester segments. The exact composition of the TPU used is a trade secret, but its structure was approximated with standard TPU structures consisting of diphenylmethanediisocyanate (MDI)/butane diol (BD) hard segment and a mixed adipate ester soft segments. Because no hard segment melting was observed in the pure TPU, it was concluded that it is a copolymer of different diols and perhaps different isocyanates. It is possible that hard segments of urethane have stronger interactions with amorphous PLA due to hydrogen bonding than the soft segment polyester, although solubility parameters of three components are close (and dependent on the method of calculation). The PLA solubility parameter is reported[29] to be 21 $(MPa)^{0.5}$, while the calculated MDI/BD hard segment is 23 $(MPa)^{0.5}$ using Van Krevelen Method or 19 $(MPa)^{0.5}$ by Hoy method, whereas polyethylene-butylene adipate was estimated to be 20 $(MPa)^{0.5}$ by Van Krevelen and 21 $(MPa)^{0.5}$ by Hoy method.[30] Such close solubility parameters create conditions for complete miscibility but entropic factors were responsible for phase separation. If the soft segment would interact strongly with PLA, then soft segment T_g would increase and PLA T_g would decrease, but only the latter occurred.

The mixture is more complex due to the presence of the unknown amount of plasticizer in TPU, probably an ester, which may also plasticize PLA. In the second DSC cycle, the PLA glass transition also shifts to lower temperatures. The melting temperature of PLA changes from 167°C for the pure PLA to 153°C for the blend with 10 wt % of PLA (Table II).

Crystallinity of the samples used for mechanical tests was calculated by subtracting enthalpy of crystallization preceding melting, ΔH_c, from the melting enthalpy, ΔH_m, divided by the mass of PLA in the sample, w_{PLA}, and equilibrium enthalpy of fusion of 100% crystalline PLA,[31] of 93 J g^{-1}:

$$\text{Crystallinity} = \frac{\Delta H_m - \Delta H_c}{w_{PLA} \times 93 J/g} \times 100\% \quad (1)$$

Pure PLA shows cold crystallization and high amorphous content. Its crystallinity is lower than in blends, due to overlapping of crystallization and melting. Similar behavior was reported by Solarski et al.[32] who separated crystallization from melting of PLA using modulated DSC. Results in Table I and Figure 4 show glass transition temperature and crystallinity of the samples as they were made (the first cycle). DMA results are also consistent with the high content of amorphous phase in PLA. Although approximately the same procedure was followed in preparing the blends, variability of experimental conditions would affect the accuracy of data. Thus the results have to be

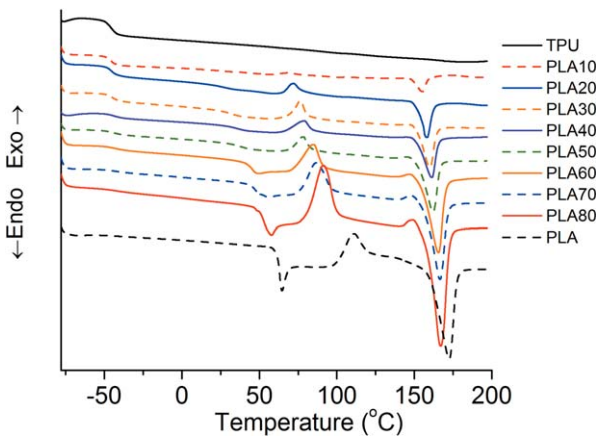

Figure 4. DSC thermograms of PLA/TPU blends and starting components (first cycle). [Color figure can be viewed in the online issue, which is available at wileyonlinelibrary.com.]

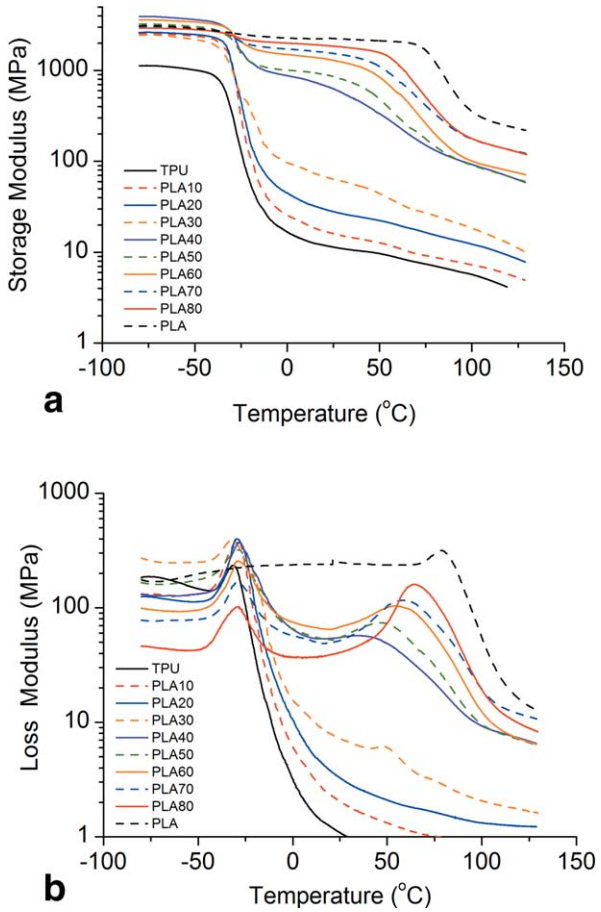

Figure 5. Storage modulus (a) and loss modulus (b) of blends with different wt % of PLA, PLA10 denotes blend with 10 wt % of PLA in the blend. [Color figure can be viewed in the online issue, which is available at wileyonlinelibrary.com.]

treated with caution as they only show the trend. Lower crystallinity was observed in samples with 70 and 80 wt % PLA, possibly due to variations in cooling conditions.

In case of miscible polymers, glass transition of a blend, T_g, shifts with composition according to Fox-Flory equation ($1/T_g = w_1/T_{g1} + w_2/T_{g2}$) where w_1 and w_2 are weight fractions of two components and T_{g1} and T_{g2} are their glass transitions. In partially miscible blends, as in our system, glass transition of PLA will be lowered depending on the amount of TPU mixed in PLA. Here T_g is the glass transitions of PLA phase in a blend and T_{g1} and T_{g2} are glass transitions of pure PLA and TPU, respectively (all temperatures are given in Kelvin). Weight fraction of TPU dissolved in PLA phase (w_2) decreases from 27 to 9% as the overall content of PLA in the blend increases from 20 to 80 wt %. This shows that TPU content dissolved in the PLA phase is considerable.

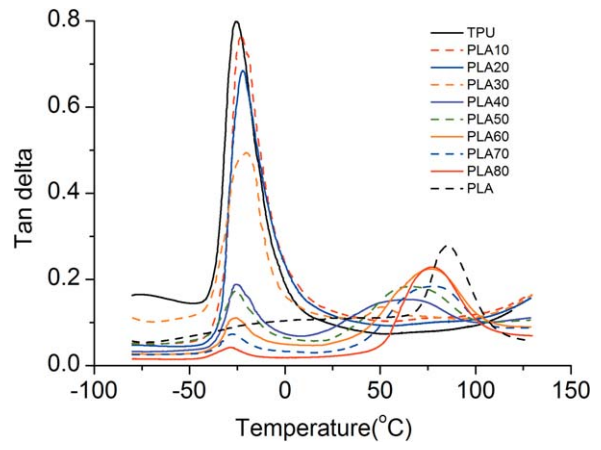

Figure 6. Tan delta of blends with different wt % of PLA. PLA10 denotes the blend with 10 wt % of PLA. [Color figure can be viewed in the online issue, which is available at wileyonlinelibrary.com.]

Table III. Glass Transition of Pure TPU, PLA, and their Blends Determined from Peaks in Tan Delta and Loss Modulus vs. Temperature Curves

	Tan delta		Loss modulus	
Sample	T_{g1} (°C)	T_{g2} (°C)	T_{g1} (°C)	T_{g2} (°C)
TPU	−25.5	-	−31.5	-
PLA-TPU 10-90	−22.9	55.5	−29.0	-
PLA-TPU 20-80	−22.3	55.2	−29.6	-
PLA-TPU 30-70	−20.6	51.1	−32.0	48.8
PLA-TPU 40-60	−25.9	64.9	−28.7	35.5
PLA-TPU 50-50	−25.9	65.5	−28.7	46.2
PLA-TPU 60-40	−25.5	76.7	−28.8	54.3
PLA-TPU 70-30	−27.5	78.0	−29.4	59.0
PLA-TPU 80-20	−28.1	77.2	−28.8	64.4
PLA	-	85.6	-	-

Dynamic Mechanical Properties

Dynamic mechanical data offer further insight into the morphology of the blends. Figure 5 displays storage moduli (E') and loss moduli (E'') change with temperature. Pure PLA displays a high modulus (~2 GPa), up to 60°C followed by a drop to about 0.5 GPa at 150°C, while pure TPU shows about two order of magnitude drop in E' at T_g (−25°C). In samples with continuous PLA phase (PLA concentrations of 40–100 wt %), the modulus is maintained at a high level up to 60°C. In samples with 10, 20, and 30 wt % PLA, the storage modulus drop between −50 and 0°C is consistent with globular morphology and TPU as a continuous phase. The results are in agreement with SEM data.

Loss modulus curves display a low temperature peak at −31°C for pure TPU and one at around 80°C for pure PLA, which are associated with T_g of TPU and PLA, respectively. While the temperature of the TPU E'' maximum is unchanged within limits of experimental error, PLA peak temperature decreases with decreasing PLA content. Tan delta curves (Figure 6) display two distinct peaks: one at about −25°C associated with the TPU glass transition, and a second at 55–85°C associated with the PLA T_g. Tan δ of the TPU component in samples with 40 wt % PLA and less, have values of 0.4–0.8, and below 0.2 for the sample with 50 wt % PLA and above. Higher tan δ values do not reflect only higher concentration of TPU in the blends, but also higher mobility associated with the continuous TPU phase structure. Low values are associated with lower mobility of soft

Table IV. Mechanical Properties of PLA, TPU, and Blends

Sample	Tensile strength (MPa)	Elongation at break (%)	Young modulus (MPa)	Shore A	Shore D	Impact strength (kJ m^{-2})
TPU	5.9 ± 1.4	630.9 ± 143	8 ± 1	69	13	-
PLA-TPU 10-90	7.5 ± 0.9	597.9 ± 92	13 ± 1	77	18	-
PLA-TPU 20-80	8.3 ± 2.1	581.8 ± 96	14 ± 2	80	20	-
PLA-TPU 30-70	7.3 ± 0.4	408.2 ± 74	12 ± 2	92	29	-
PLA-TPU 40-60	9.8 ± 0.7	112.8 ± 52	138 ± 7	95	49	-
PLA-TPU 50-50	11.5 ± 0.1	50.2 ± 38	388 ± 5	-	60	-
PLA-TPU 60-40	17.5 ± 0.9	34.7 ± 23	529 ± 4	-	67	8.9 ± 0.8
PLA-TPU 70-30	22.2 ± 1.6	14.2 ± 4	763 ± 8	-	71	7.3 ± 0.1
PLA-TPU 80-20	31.3 ± 0.8	10.3 ± 5	1118 ± 15	-	77	5.9 ± 0.2
PLA	44.8 ± 9.3	4.3 ± 1	1496 ± 20	-	85	3.4 ± 0.6

segments in TPU confined in the rigid continuous PLA phase. Fairly large tan δ at the PLA transition at 85°C indicates high content of the amorphous phase in PLA, presumably due to fast cooling and slow crystallization (Table III).

Mechanical Properties

Mechanical properties strongly depend on the blend composition and morphology (Table IV). Stress-strain curves of blends exhibit gradual change from elastic behavior of TPU to stiff materials with curves that are characterized by a yield point (Figure 7). Blends with 0–40 wt % PLA show typical elastomeric behavior and no yield points. The curves for samples with 70–100 wt % PLA show strong yield points at elongations of several percent, followed by a significant drop in stress at higher elongations, characteristic of a continuous rigid PLA phase. Plotting mechanical properties versus composition shows more clearly the influence of morphology. Figure 8 shows almost constant elongation of about 600% for pure polyurethane and blends with 10 and 20 wt % PLA, and elongations below 15% for samples with 70 to 100 wt % PLA, suggesting the discontinuous PLA structure in the former and discontinuous TPU phase in the latter. Thus, co-continuous structures are possible in 30–60 wt % PLA composition range. Modulus increases almost linearly with increasing PLA concentration from 30 to 100 wt %. Tensile strength of elastomers increases with PLA content from 0 to 30 wt %, indicating that PLA is a reinforcing agent even in samples with dispersed morphology. Further increase in PLA content brings a jump in strength and parallels increase of modulus because PLA becomes a continuous phase. The samples with 10–40 wt % PLA can be classified as hard elastomers while those above this concentration would be tough plastics.

Blends with higher content of PLA also have higher hardness. The addition of the TPU component to PLA can improve impact resistance (Table IV). We have measured impact resistance of blends with up to 40 wt % of TPU. Samples made from blends with higher TPU content are elastic materials and could not be broken. Results in this section show that with the right weight ratio of two polymers, one can tailor material properties to obtain desirable combination of hardness, improved impact resistance and good tensile properties.

CONCLUSIONS

The polyurethane used in this work is compatible with PLA even without compatibilizers. The blends with 10–40 wt % PLA

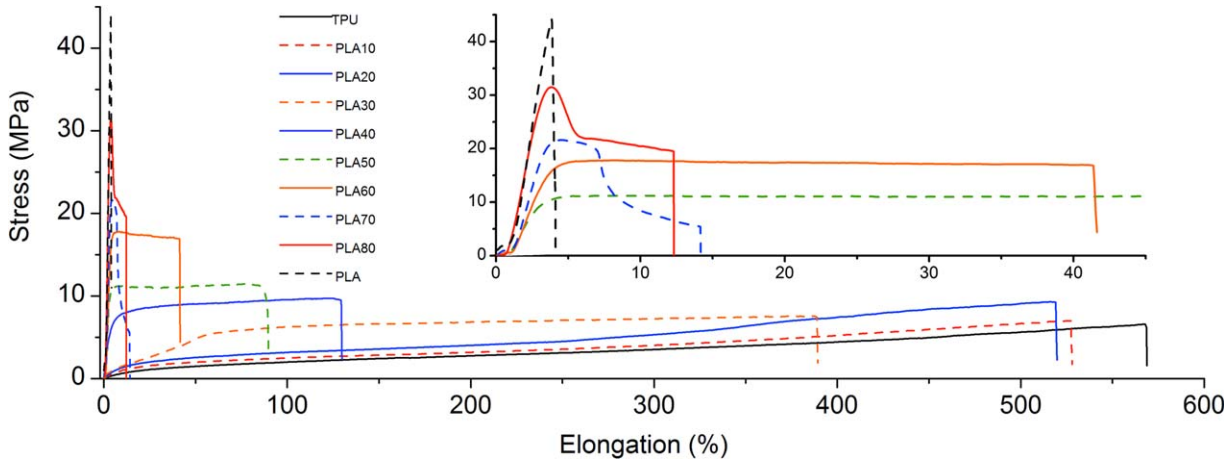

Figure 7. Stress–strain curves of pure TPU and PLA and their blends. [Color figure can be viewed in the online issue, which is available at wileyonlinelibrary.com.]

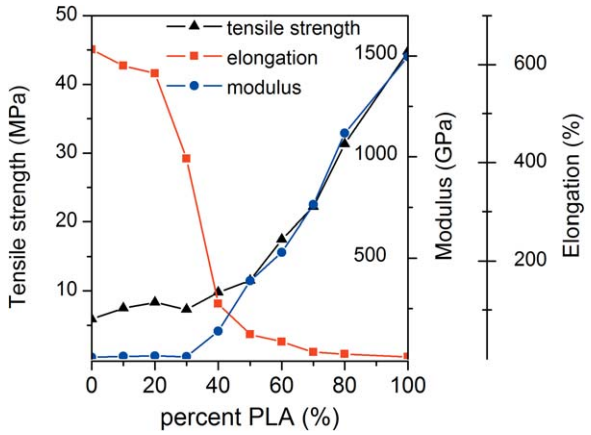

Figure 8. The effect of composition on mechanical properties of PLA/TPU blends. [Color figure can be viewed in the online issue, which is available at wileyonlinelibrary.com.]

are hard, reinforced elastomers, while those with 60–80 wt % PLA are tough plastics. Cocontinuous morphology was suggested in composition range between 40 and 60 wt % PLA. Suggested inversion points were above 30 wt % PLA (from globular PLA phase dispersed in TPU matrix to a cocontinuous morphology) and somewhere between 50 and 60 wt % PLA (a transition from cocontinuous to TPU dispersed in the PLA matrix).

Glass transition and melting point of PLA decrease, but apparent crystallinity seems to increase with decreasing PLA content in the blends. Miscibility of the blends seems to increase with increasing polyurethane content.

Tensile strength steadily increases from 6 to 44 MPa with increasing PLA content from 0 to 100 wt %, while elongation decreases from 630 to 4%, displaying precipitous drop at 40 wt % PLA, indicating inversion of morphology. Impact strength increases from 3.4 to 8.9 kJ m^{-2} by increasing polyurethane content from zero to 40 wt %. Compositions with zero to 40 wt % PLA are rubbers with increasing Shore A hardness of 70–95. New materials are potentially biodegradable with applications in the medical field.

ACKNOWLEDGMENTS

This work was supported by a grant from the United States Department of Agriculture (USDA-CSREES 2010–38924-20706). Research was carried out in collaboration of University of Novi Sad (projects III 45022 and OI 171015, Ministry of Education, Science and Technological Development of the Republic of Serbia) and Pittsburg State University.

REFERENCES

1. Hong, H.; Wei, J.; Yuan, Y.; Chen, F. P.; Wang, J.; Qu, X.; Liu, C. S. *J. Appl. Polym. Sci.* **2011**, *121*, 855.
2. Zhao, X.; Ye, L.; Coates, P.; Caton-Rose, F.; Martyn, M. *Polym. Adv. Technol.* **2013**, *24*, 853.
3. Mehta, R.; Kumar, V.; Bhunia, H.; Upadhyay, S. N. *J. Macromol. Sci. Polym. Rev.* **2005**, *45*, 325.
4. Debus, E. S.; Geiger, D.; Sailer, M.; Ederer, J.; Thiede, A. *Eur. Surg. Res.* **1997**, *29*, 52.
5. Okada, H.; Heya, T.; Igari, Y.; Ogawa, Y.; Toguchi, H.; Shimamoto, T. *Int. J. Pharm.* **1989**, *54*, 231.
6. Han, J. J.; Huang, H. X. *J. Appl. Polym. Sci.* **2011**, *120*, 3217.
7. Simmons, A.; Hyvarinen, J.; Poole-Warren, L. *Biomaterials* **2006**, *27*, 4484.
8. Cao, Q.; Cai, Y.; Jing, B.; Liu, P. *J. Appl. Polym. Sci.* **2006**, *102*, 5266.
9. Lebedev, E. V.; Ishchenko, S. S.; Denisenko, V. D.; Dupanov, V. O.; Privalko, E. G.; Usenko, A. A.; Privalko, V. P. *Compos. Sci. Technol.* **2006**, *66*, 3132.
10. Gogolewski, S.; Gorna, K.; Turner, A. S. *J. Biomed. Mater. Res. A* **2006**, *77*, 802.
11. Lamba, N. M. K.; Woodhouse, K. A.; Cooper, S. L. Polyurethanes in Biomedical Applications; CRC Press: Boca Raton, FL, **1998**.
12. Gunatillake, P. A.; Meijs, G. F.; McCarthy, S. J.; Adhikari, R. *J. Appl. Polym. Sci.* **2000**, *76*, 2026.
13. Ajili, S. H.; Ebrahimi, N. G.; Khorasani, M. T. *Iran. Polym. J.* **2003**, *12*, 179.
14. Anderson, K. S.; Hillmyer, M. A. *Polymer* **2004**, *45*, 8809.
15. Ishida, S.; Nagasaki, R.; Chino, K.; Dong, T.; Inoue, Y. *J. Appl. Polym. Sci.* **2009**, *113*, 558.
16. Huneault, M. A.; Li, H. *Polymer* **2007**, *48*, 270.
17. Sarazin, P.; Li, G.; Orts, W. J.; Favis, B. D. *Polymer* **2008**, *49*, 599.
18. Liu, X.; Dever, M.; Fair, N.; Benson, R. S. *J. Environ. Polym. Degrad.* **1997**, *5*, 225.
19. Shibata, M.; Inouea, Y.; Miyoshib, M. *Polymer* **2006**, *47*, 3557.
20. Noda, I.; Satkowski, M. M.; Dowrey, A. E.; Marcott, C. *Macromol. Biosci.* **2004**, *4*, 269.
21. Schreck, K. M.; Hillmyer, M. A. *J. Biotechnol.* **2007**, *132*, 287.
22. Robertson, M. L.; Chang, K.; Gramlich, W. M.; Hillmyer, M. A. *Macromolecules* **2010**, *43*, 1807.
23. Stoclet, G.; Seguela, R.; Lefebvre, J.-M. *Polymer* **2011**, *52*, 1417.
24. Nijenhuis, A. J.; Colstee, E.; Grijpma, D. W.; Pennings, A. *J. Polymer* **1996**, *37*, 5849.
25. Kang, H.; Qiao, B.; Wang, R.; Wang, Z.; Zhang, L.; Ma, J.; Coates, P. *Polymer* **2013**, *54*, 2450.
26. Feng, F.; Ye, L. *J. Appl. Polym. Sci.* **2011**, *119*, 2778.
27. Lai, S.-M.; Lan, Y.-C. *J. Polym. Res.* **2013**, *20*, 1.
28. Imre, B.; Renner, K.; Pukánszky, B. *Express Polym. Lett.* **2014**, *8*, 2.
29. Brandrup, J.; Immergut, E. H.; Grulke, E. A. Polymer Handbook; Wiley: New York, **1999**.
30. Krevelen, D. W. V. Properties of Polymers; Elsevier: New York, **1990**.
31. Fischer, E. W.; Sterzel, H. J.; Wegner, G. *Colloid. Polym. Sci.* **1973**, *251*, 980.
32. Solarski, S.; Ferreira, M.; Devaux, E. *Polymer* **2005**, *46*, 11187.